Single-Molecule Magnets (SMMs): A Molecular (Bottom-up) Approach to Nanoscale Magnetic Materials

Lecture 2:
The Mn_4 and $[Mn_4]_2$ Family of SMMs

George Christou
Department of Chemistry, University of Florida
Gainesville, FL 32611-7200, USA

Advantages of SMMs over Traditional Nanoscale Magnetic Particles

Properties

- truly monodisperse particles of nanoscale dimensions
- crystalline, therefore contain highly ordered assemblies
- well-defined ground state spin, S
- truly quantum spin systems

Synthesis

- synthesized by room temperature, solution methods
- enveloped in a protective shell of organic groups (ligands)
- truly soluble (rather than colloidal suspensions) in organic solvents
- the organic shell (ligands) around the magnetic core can be easily modified, providing control of separations between molecules, coupling with the environment, etc.

Major Potential Applications of SMMs

Digital Information Storage

- the storage of information at the molecular level as the orientation direction of the magnetization vector.
- each molecule stores one bit of information.
- estimated 10^4 increase in storage density over present devices.
- requires ordered arrays of SMMs, either 2-D surfaces (present technology) or 3-D crystals (future technology).

Quantum Computing

- the use of quantum bits (qubits) rather than classical bits as in present computation methods.
- requires SMMs capable of existing in quantum superpositions of two (or more) states i.e. 1 and 0 instead of classical 1 or 0.
- requires SMM to show appropriate quantum properties.

Topics for this presentation:

- Crystalline arrays of Mn_4 SMMs, and their controlled modification.
- Supramolecular dimers of Mn_4 SMMs: exchange-biased quantum tunnelling

The Mn_{12} Family of Single-Molecule Magnets (SMMs)

$Mn(O_2CMe)_2$ + MnO_4^- in 60% $MeCO_2H/H_2O$ ⟶ $[Mn_{12}O_{12}(O_2CMe)_{16}(H_2O)_4]$ (Lis, 1980)

$[Mn_{12}Ac]\cdot 2AcOH\cdot 4H_2O$

Identified as a SMM in 1993. $Mn_{12}Ac$ has axial symmetry (tetragonal space group *I*4(bar)), and has therefore been considered the best to study in detail.

$[Mn_{12}O_{12}(O_2CR)_{16}(H_2O)_4]$ (Mn_{12}) complexes:

- **S = 10**
- **D = -0.40 to -0.50 cm^{-1} (-0.58 to -0.72 K)**
- **Magnets below 3K**

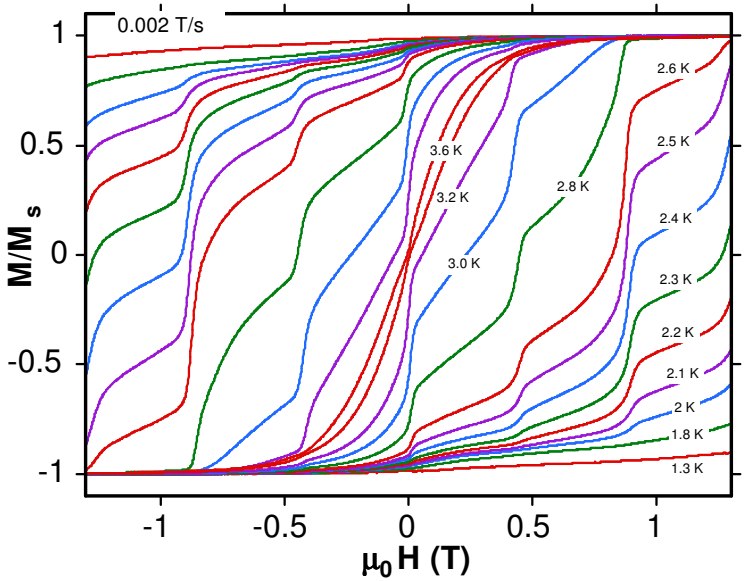

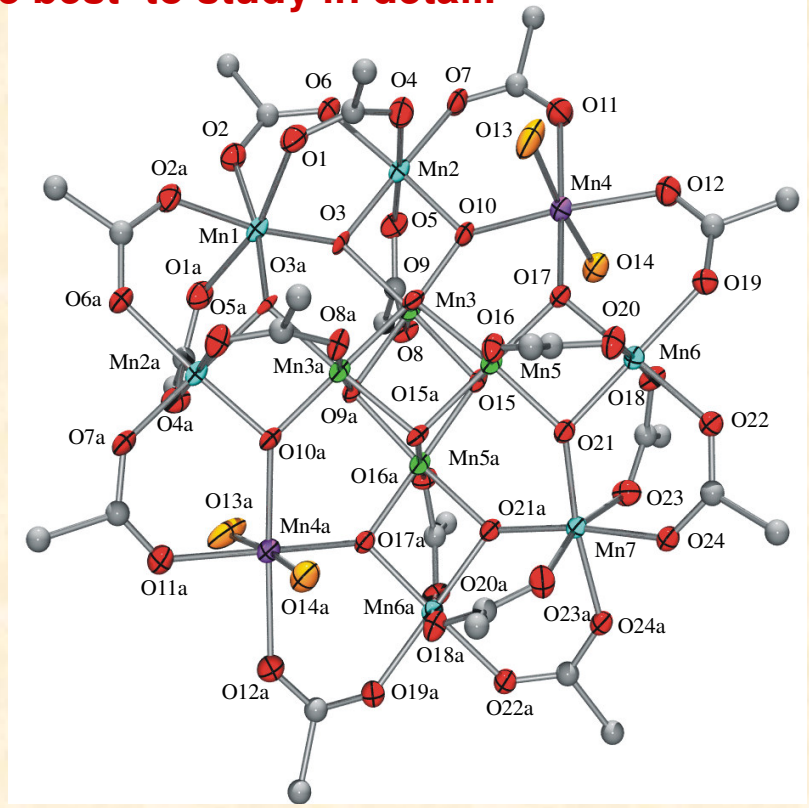

Volume of the $Mn_{12}O_{12}$ magnetic core ~ 0.1 nm^3

Distorted-Cubane Mn_4 SMMs with $S = 9/2$

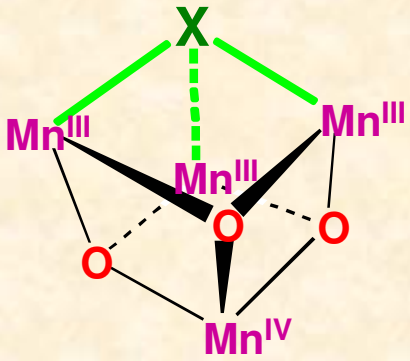

- $3Mn^{III}$, Mn^{IV} (trapped valence)
- C_{3v} virtual core symmetry
- Mn^{3+} Jahn-Teller axial elongations
- Core ligands (X): Cl^-, Br^-, F^-, NO_3^-, N_3, NCO^-, OH^-, MeO^-, Me_3SiO^-, $MeCO_2^-$, $PhCO_2^-$

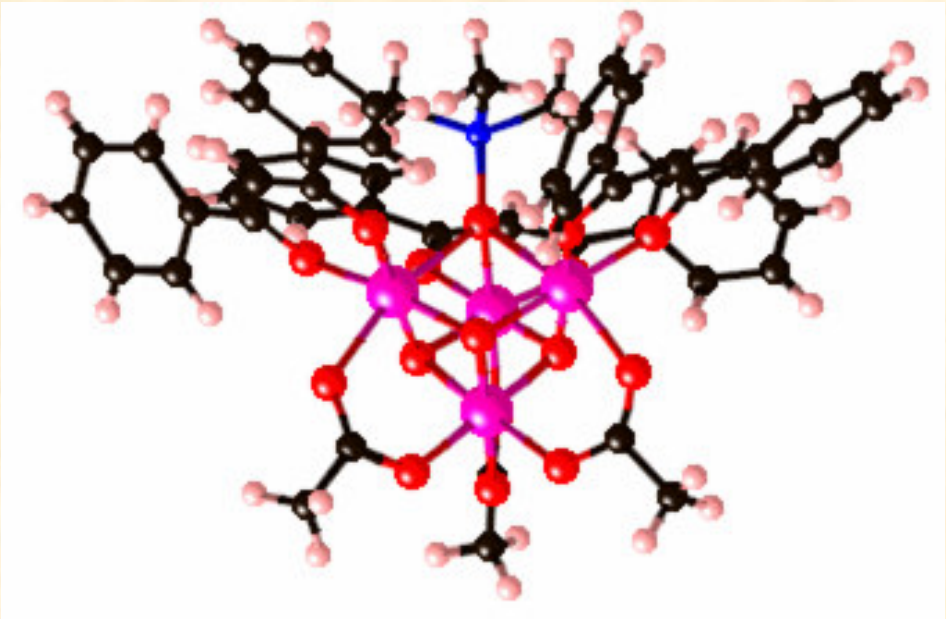

Advantages of the Mn_4 family

- Variation in core X group, for given organic groups
- Variation in organic groups, for a given Mn_4O_3X core.
- Soluble and crystalline
- Mn_4O_3X core volume ~ 0.01 nm^3

Properties of Mn_4 SMMs

- $S = {}^{9}/_{2}$
- $D = -0.65$ to -0.75 K
- $U = \Delta E = (S^2 - {}^{1}/_{4})|D| = 20$ D

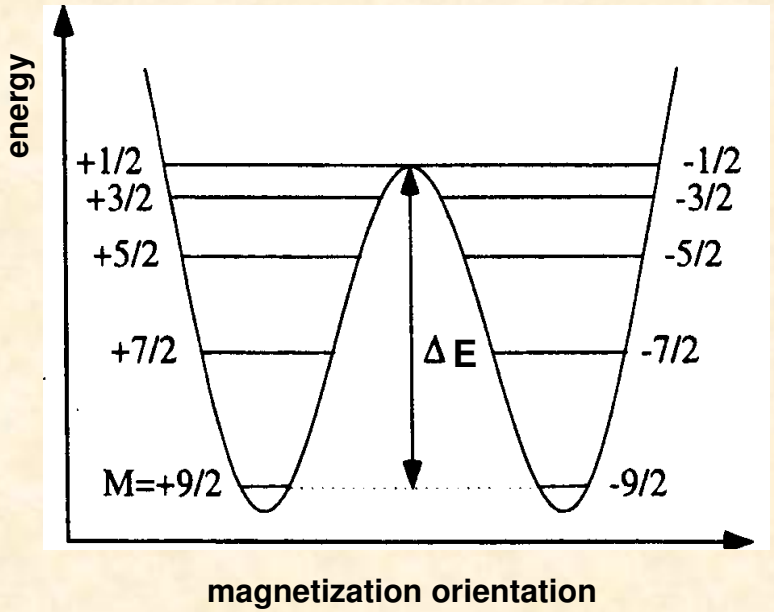

X	$OSiMe_3$
J_{34} (cm^{-1})	-34.35
J_{33} (cm^{-1})	+13.41
g	1.97
S	9/2
1st ex. state	264 cm^{-1}

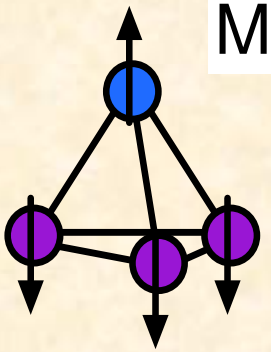

Mn^{IV} $S_1 = 3/2$

Mn^{III} $S_2 = 2$

S = 9/2

$\mathcal{H} = -2J\,\hat{S}_i \cdot \hat{S}_j$ convention

AC Susceptibility and Magnetization Hysteresis

-- for low-symmetry (triclinic)
$Mn_4O_3Cl(O_2CMe)_3(dbm)_3$

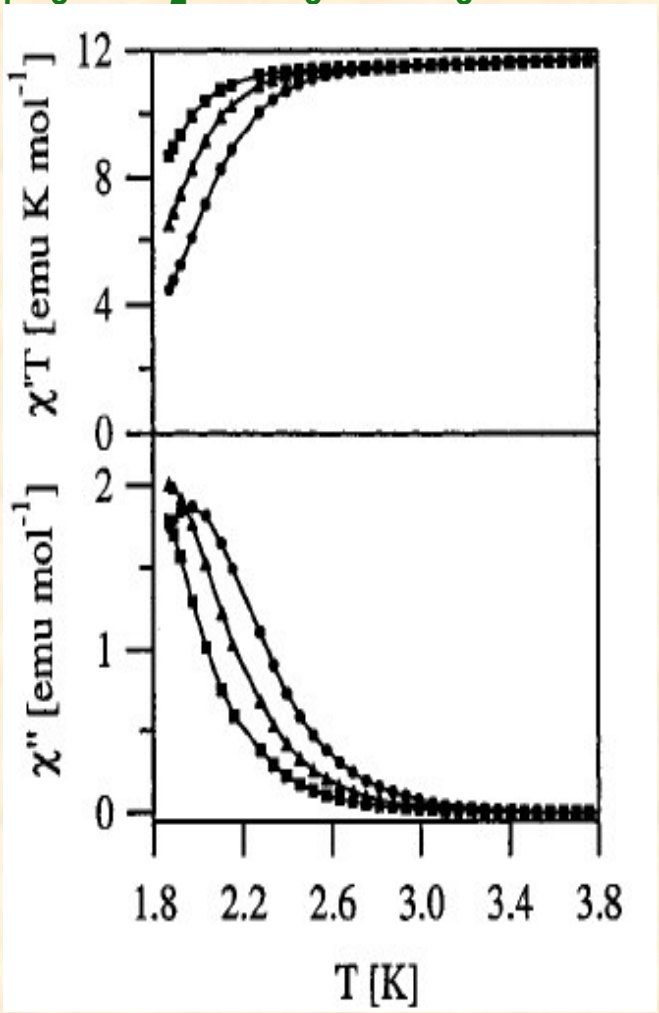

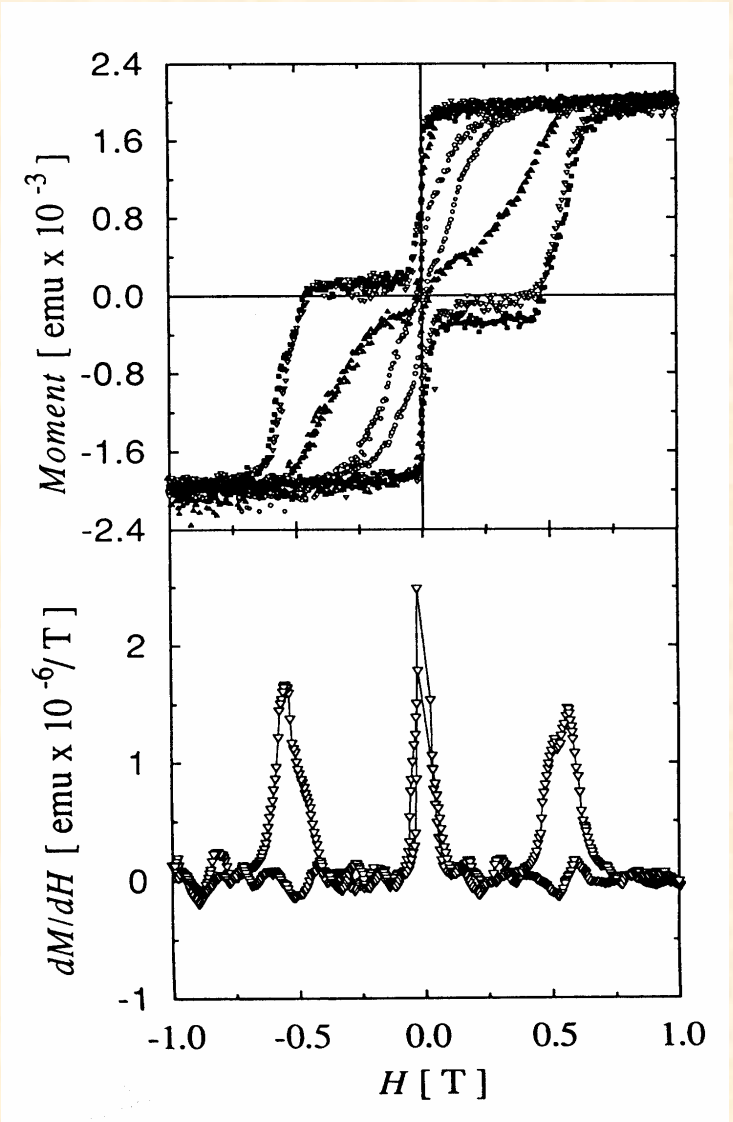

Arrhenius Plot for Axial (Hexagonal Space Group) Mn_4 (X = $OSiMe_3$) with $S = 9/2$

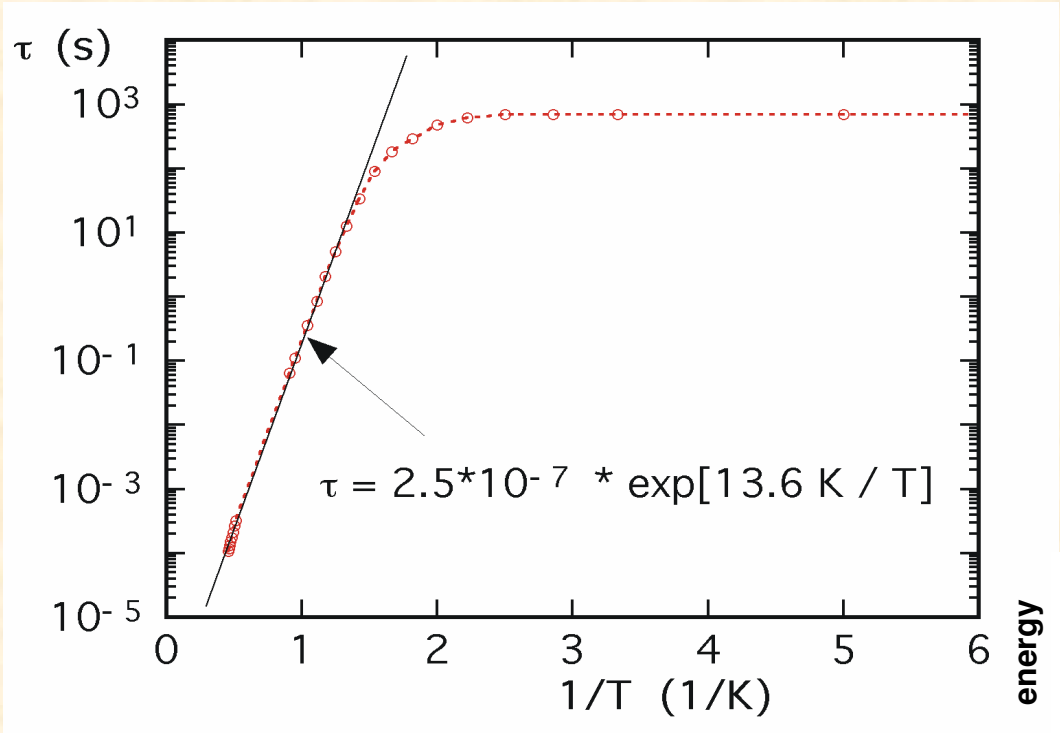

Arrhenius Plot from magnetization decay vs time data

$1/\tau = (1/\tau_o) \exp(-U_{eff}/kT)$

Arrhenius barrier Δ (i.e. U_{eff}) = 13.6 K

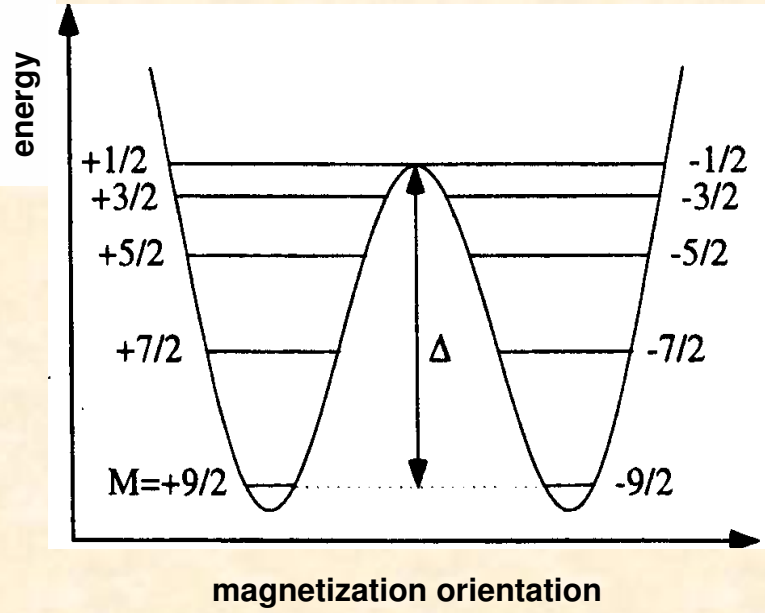

Below 0.5 K, temperature-independent relaxation via ground state tunnelling (unpublished)

Summary of Properties of Selected Mn_4 Complexes Obtained from DC Magnetization Fits

X	Cl	Br	$MeCO_2$	
J_{34} (cm^{-1}) [a]	-28.4	-30.1	-33.9	
J_{33} (cm^{-1}) [a]	+8.3	+7.4	+5.4	
Ground State	9/2	9/2	9/2	
1st Excited State	7/2	7/2	7/2	
D cm^{-1} (K)	-0.53 (-0.76)	-0.50 (-0.72)	-0.47 (-0.68)	
ΔE (S = 7/2), K	266	257	240	

[a] Using the $-2J\hat{S}_i \cdot \hat{S}_j$ convention. Change sign and double for $J\hat{S}_i \cdot \hat{S}_j$

Inelastic Neutron Scattering Studies of $[Mn_4O_3X(OAc)_3(dbm)_3]$ (X = Br, Cl, Ac, and F): Variation of the Anisotropy along the Series

H. Andres et al., *J. Am. Chem. Soc.* 2000, *122,* 12469-12477

-- on 4g each of non-deuterated samples!

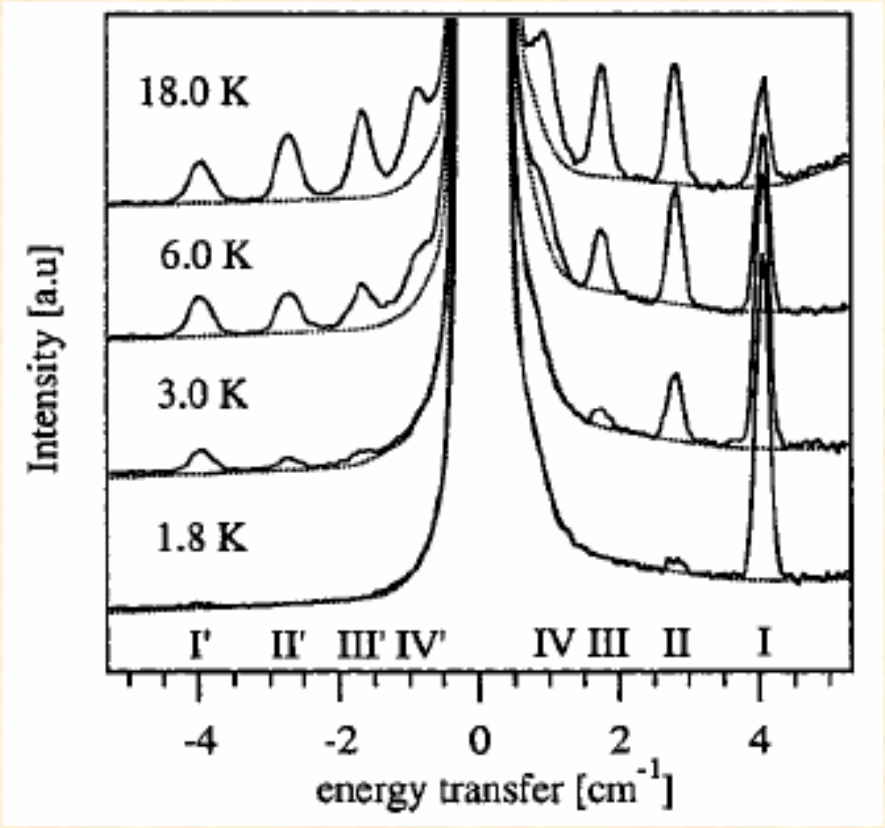

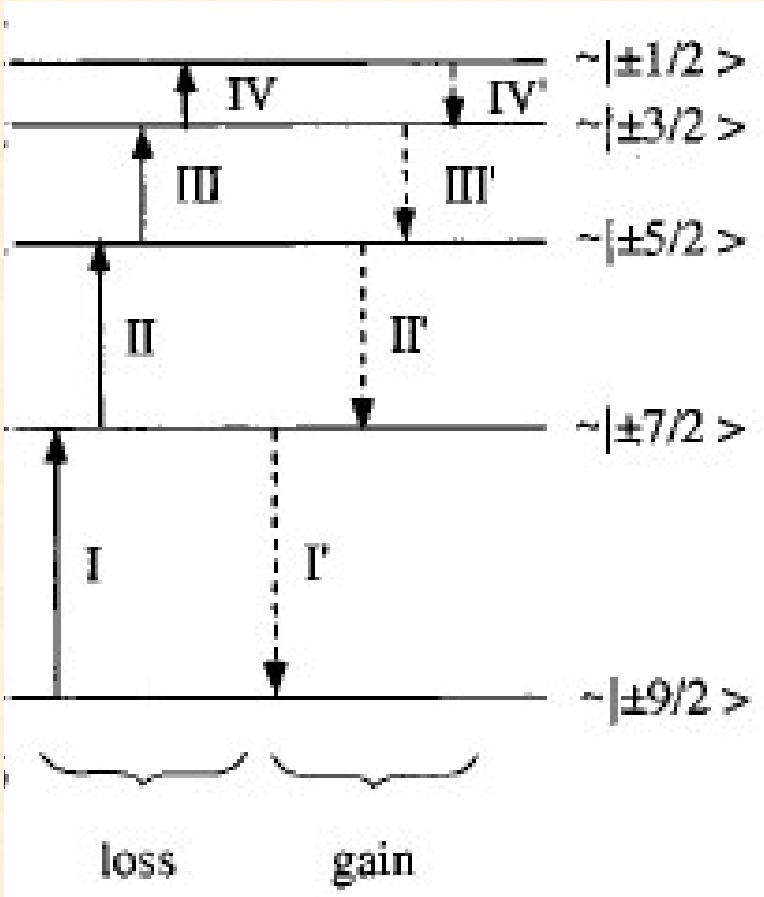

$$\hat{H}_{ZFS} = D_{cluster}[\hat{S}_z^2 - \tfrac{1}{3}S(S+1)] + E_{cluster}(\hat{S}_x^2 - \hat{S}_y^2) + B_4^0\hat{O}_4^0$$

where $\hat{O}_4^0 = 35\hat{S}_z^4 - 30S(S+1)\hat{S}_z^2 + 25\hat{S}_z^2 + 6S(S+1)$.

T = 18 K

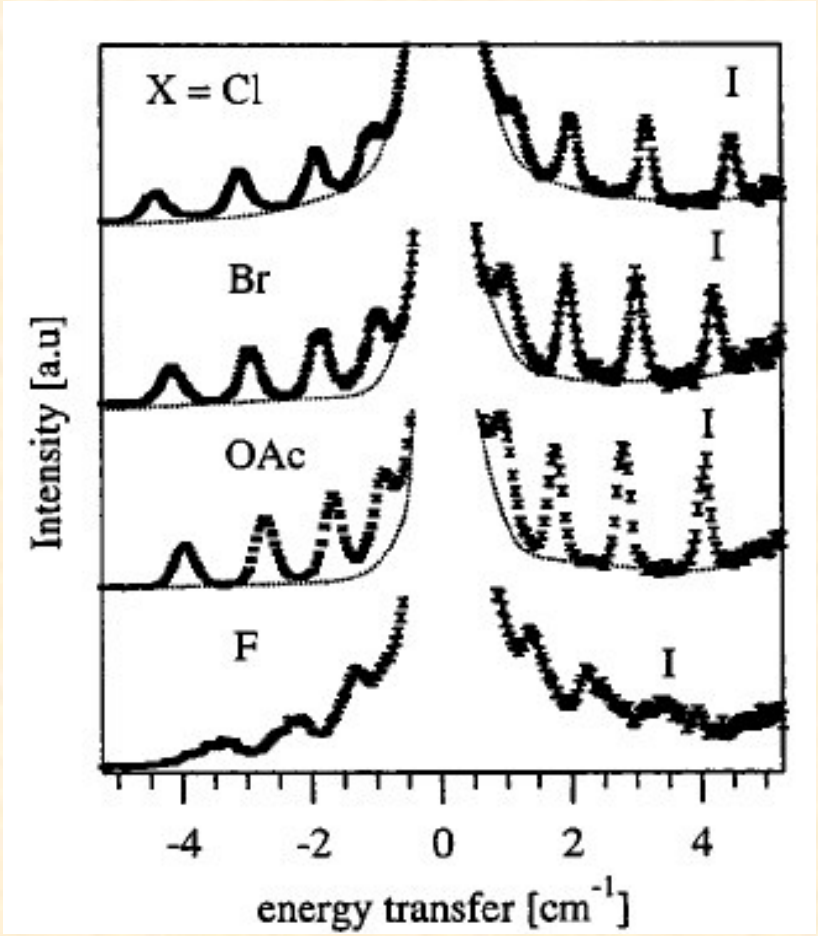

X	D [cm^{-1}] cluster	$\lvert E\rvert$ [cm^{-1}] cluster	B_4^0 [10^{-5} cm^{-1}] cluster
Cl	−0.529	0.022	−6.5
Br	−0.502	0.017	−5.1
OAc	−0.469	0.017	−7.9
F	−0.379	-	−11.1

Comparison of Data from Magnetization Fits and INS Studies

A. From Magnetization Fits:

X	Cl	Br	$MeCO_2$	
J_{34} (cm^{-1})	-28.4	-30.1	-33.9	
J_{33} (cm^{-1})	+8.3	+7.4	+5.4	
Ground State	9/2	9/2	9/2	
1st Excited State	7/2	7/2	7/2	
D cm^{-1} (K)	-0.53 (-0.76)	-0.50 (-0.72)	-0.47 (-0.68)	
ΔE (S = 7/2), K	266	257	240	

B. From Inelastic Neutron Scattering: *J. Am. Chem. Soc.* **2000**, *20*, 12469

X	Cl	Br	$MeCO_2$	F	Me_3SiO[a]
D(cm^{-1})	-0.529	-0.502	-0.469	-0.379	-0.487
$\|E\|$(cm^{-1})	0.022	0.017	0.017	-	0.011
B_4^o (cm^{-1}) x 10^5	-6.5	-5.1	-7.9	-11.1	-6.5
U_{eff}	10.66	10.10	9.43	7.59	9.77

a. crystallographic axial (C_3) symmetry

Hysteresis loops for Axial Mn_4 (X = $OSiMe_3$) with S = 9/2

$$\mathcal{H} = -D\,\hat{S}_z^2 + \mathcal{H}^{trans} + g\,\mu_B\,\mu_0\,\hat{S}\,H$$

$(2S_i + 1)$ energy states

$S = 9/2$: **10** energy states

$M_S = -S, -S+1, \ldots, S$

$D = X g\mu_B/k_B$ (**X** is the step separation)

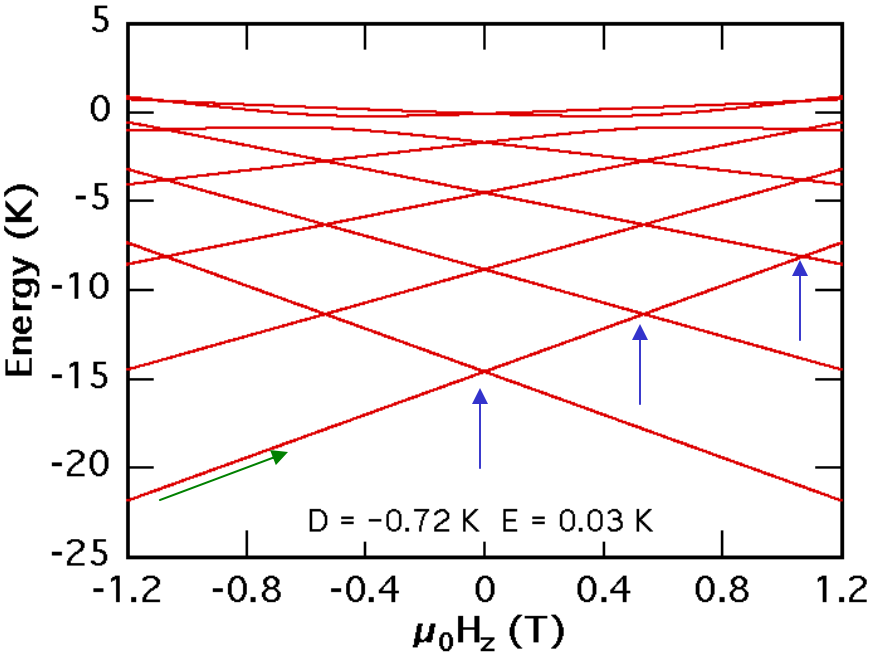

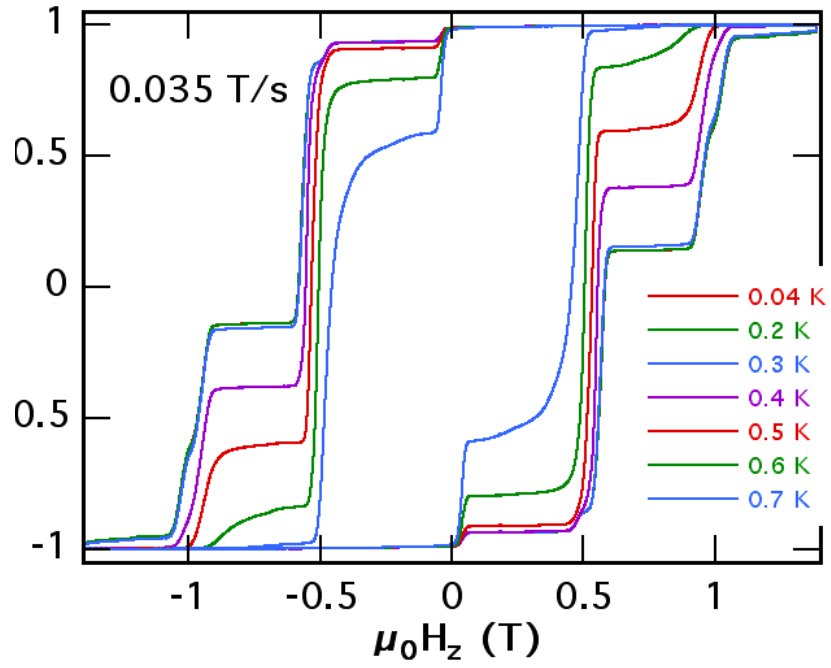

Intermolecular Interactions in Mn_4Si

Z axis
(C_3 axis)

..... are C-H···O hydrogen-bonds

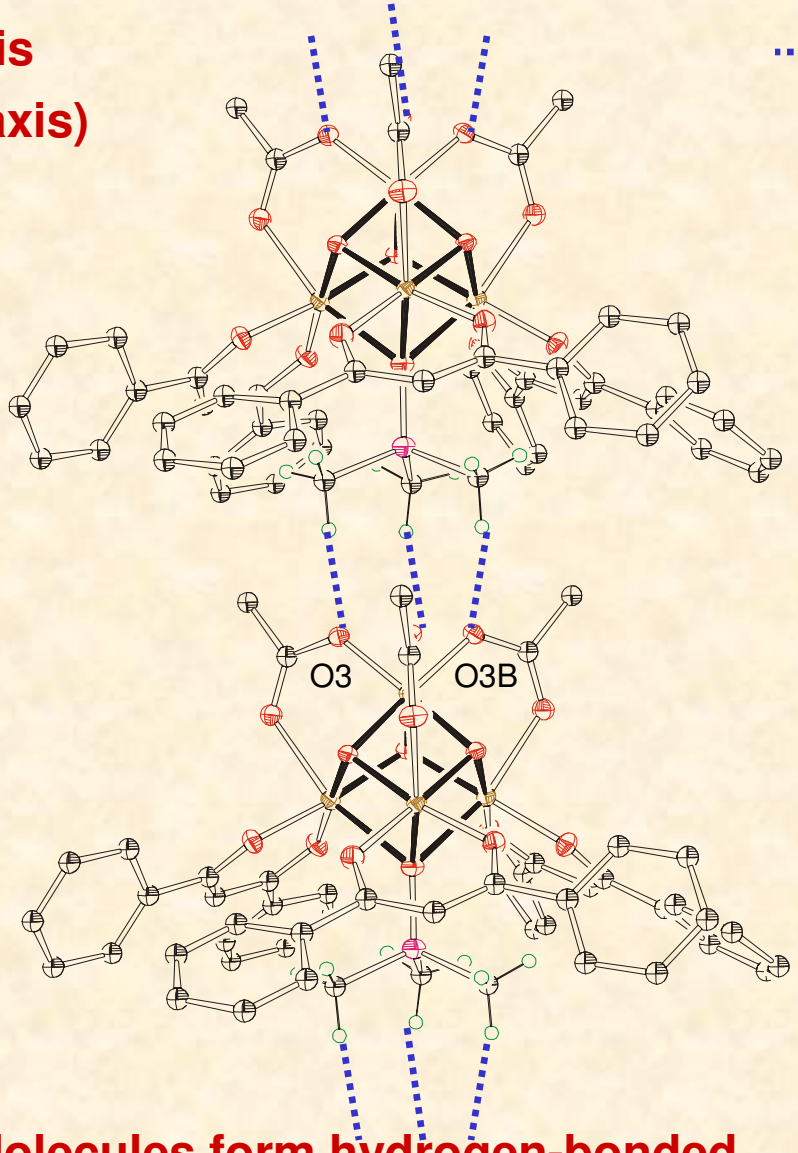

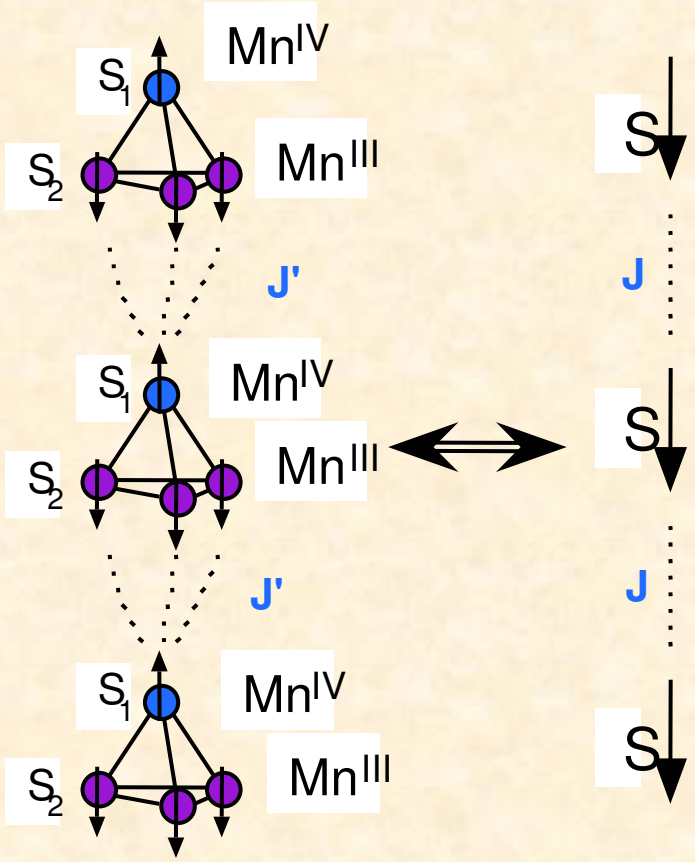

Molecules form hydrogen-bonded chains (along the crystal c axis)

Inter-Mn_4 coupling $JS^2 \approx 0.025K$

Dipolar component ≈ 0.007 K

Very Low Symmetry Mn_4 SMMs with $S = 9/2$

Only C_S symmetry --- in contrast to approx. C_{3V} of other Mn_4 SMMs

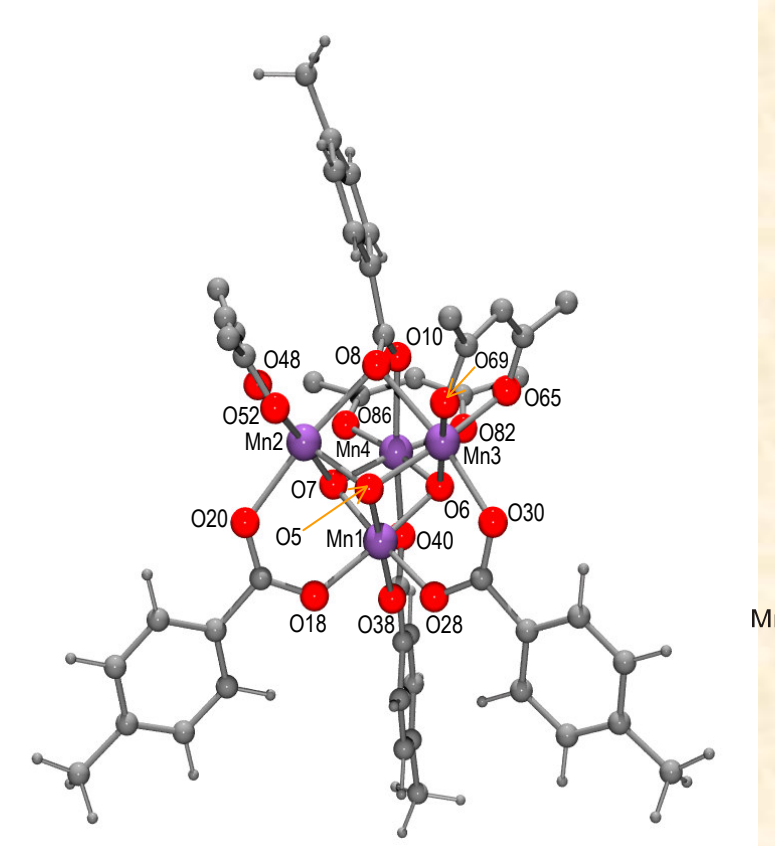

Variable group

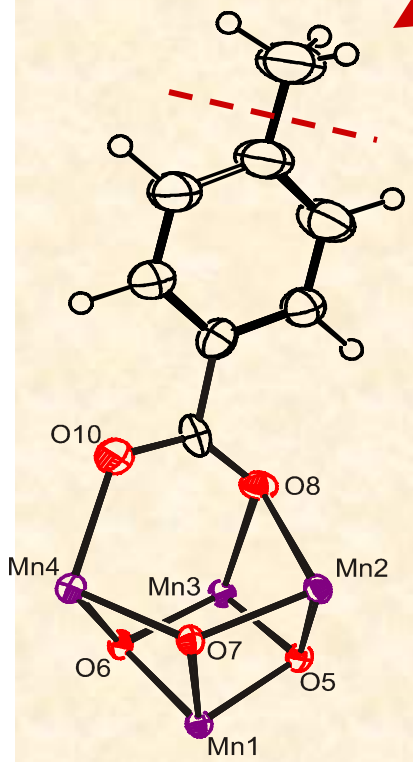

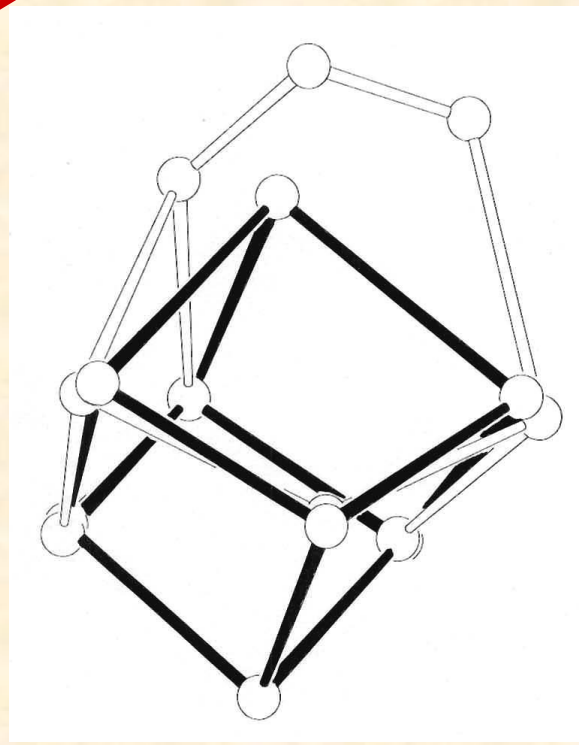

N. Aliaga-Alcalde, W. Wernsdorfer, S.Hill. G. Christou, et al., *JACS,* 2002, *126*, 12503

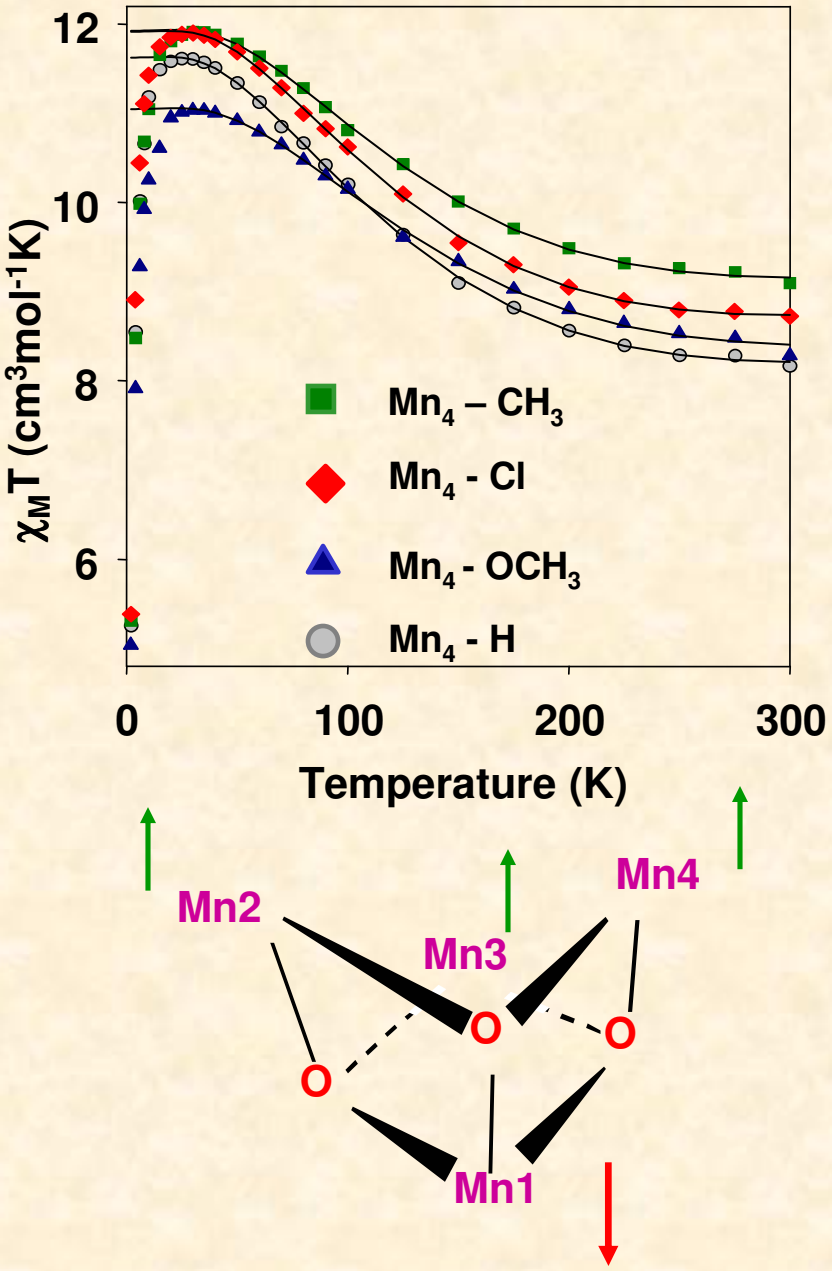

The isotropic Heisenberg spin Hamiltonian for C_S symmetry Mn_4

$$\mathcal{H} = -2J(\hat{S}_1\cdot\hat{S}_2 + \hat{S}_1\cdot\hat{S}_3 + \hat{S}_1\cdot\hat{S}_4) - 2J_a(\hat{S}_2\cdot\hat{S}_4 + \hat{S}_3\cdot\hat{S}_4) - 2J_b(\hat{S}_3\cdot\hat{S}_4)$$

where $J = J(Mn^{3+}/Mn^{4+})$

$J_a = J(Mn^{3+}/Mn^{3+})$

$J_b = J(Mn^{3+}/Mn^{3+})$

The fits give:

J = -22.9 to -27.4 cm^{-1}

J_a = + 3.2 to + 4.9 cm^{-1}

J_b = +0.5 to +0.81 cm^{-1}

All have S = 9/2 ground state

$|S, S_A, S_B\rangle = |9/2, 6, 3/2\rangle$

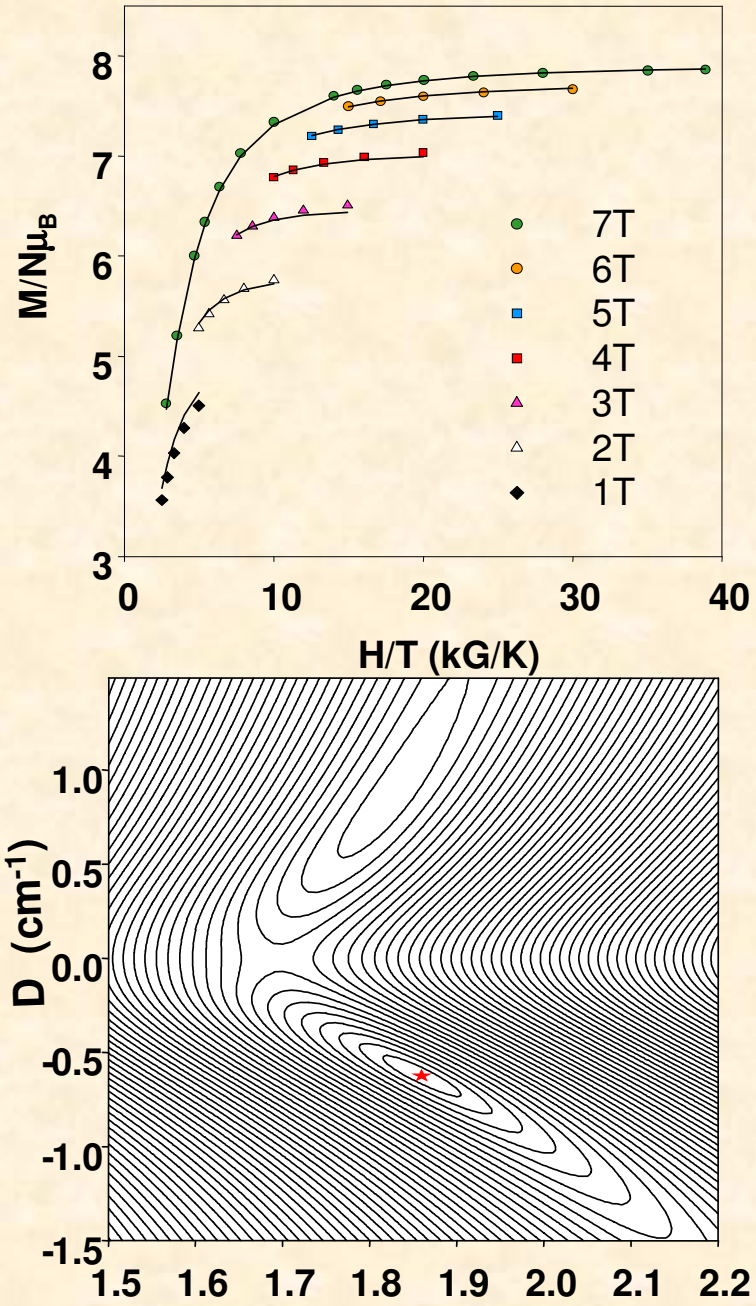

Magnetization vs DC Field and Temperature Fits

	D (cm^{-1})	g	S
Mn_4 - H	- 0.60	1.95	9/2
Mn_4 - CH_3	- 0.62	1.92	9/2
Mn_4- OCH_3	- 0.62	1.85	9/2
Mn_4 - Cl	- 0.65	1.96	9/2
$Mn_4O_3(O_2CCH_3)_4(dbm)_3$ approx C_{3V} symmetry	- 0.35	1.99	9/2

Comparison of Low-/High- Symmetry Mn_4 Complexes

A. From Magnetization Fits:

Low

X	Cl	Br	$MeCO_2$	$PhCO_2$ (-H)
J_{34} (cm^{-1})	-28.4	-30.1	-33.9	-28.5
J_{33} (cm^{-1})	+8.3	+7.4	+5.4	+2.8
J_{33} (cm^{-1})	-	-	-	+2.1
Ground State	9/2	9/2	9/2	9/2
1st Excited State	7/2	7/2	7/2	7/2
D cm^{-1} (K)	-0.53 (-0.76)	-0.50 (-0.72)	-0.47 (-0.68)	-0.60 (-0.86)
ΔE (S = 7/2), K	266	257	240	164

B. From Inelastic Neutron Scattering: ***J. Am. Chem. Soc.* 2000, *20*, 12469**

X	Cl	Br	$MeCO_2$	F	Me_3SiO[a]
D(cm^{-1})	-0.529	-0.502	-0.469	-0.379	-0.487
$\|E\|$(cm^{-1})	0.022	0.017	0.017	-	0.011
B_4^o (cm^{-1})[b]	-6.5	-5.1	-7.9	-11.1	-6.5
U_{eff}	10.66	10.10	9.43	7.59	9.77

High-Frequency EPR Studies on $Mn_4 - CH_3$

Powder spectrum at 249 GHz

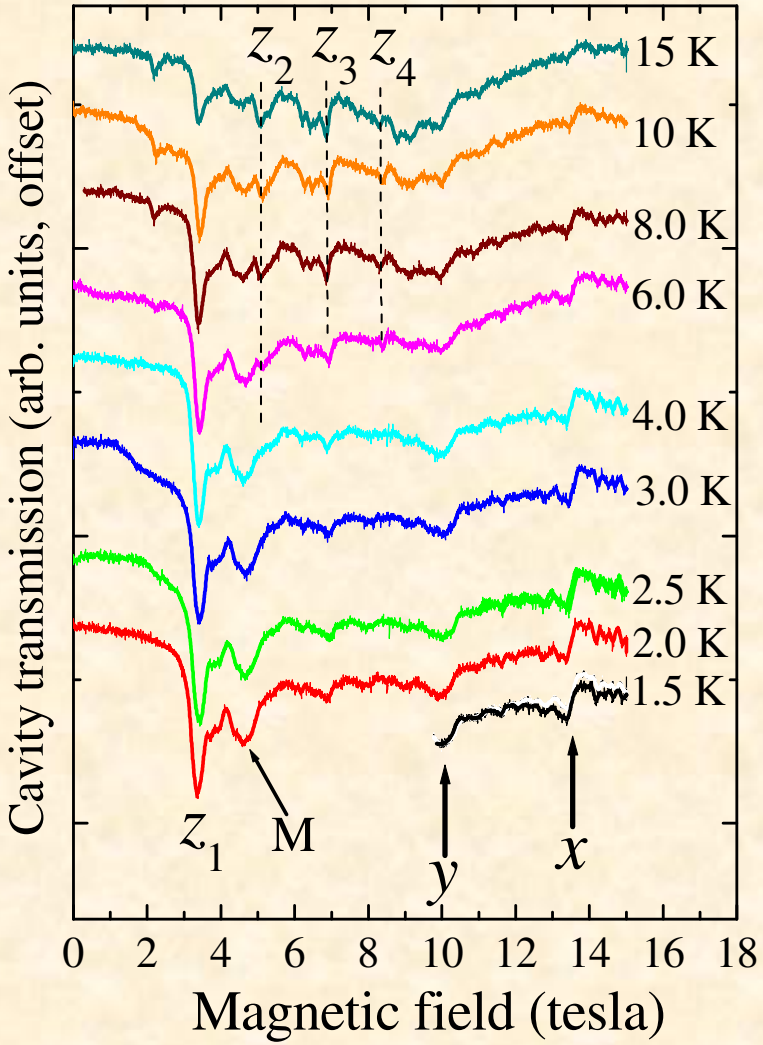

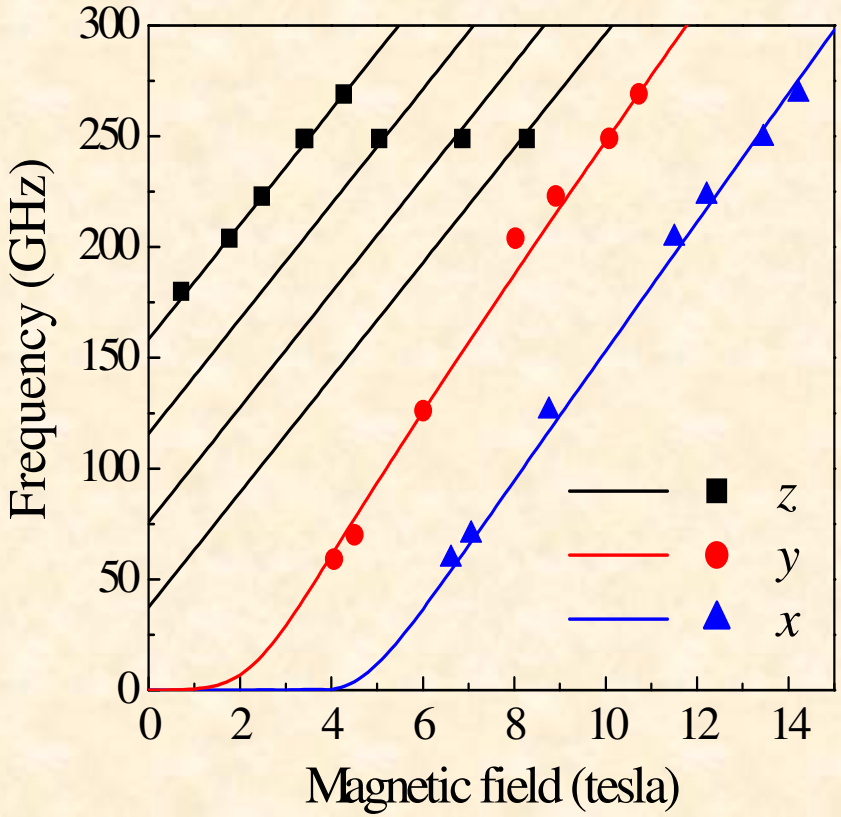

$D = -0.646\ cm^{-1}$, $|E| = 0.140\ cm^{-1}$

$B_4^0 = -3.5 \times 10^{-5}\ cm^{-1}$

N. Aliaga-Alcalde, W. Wernsdorfer, S. O. Hill, G. Christou, et al., *JACS*, 2002, *126*, 12503

Magnetization Hysteresis Loops

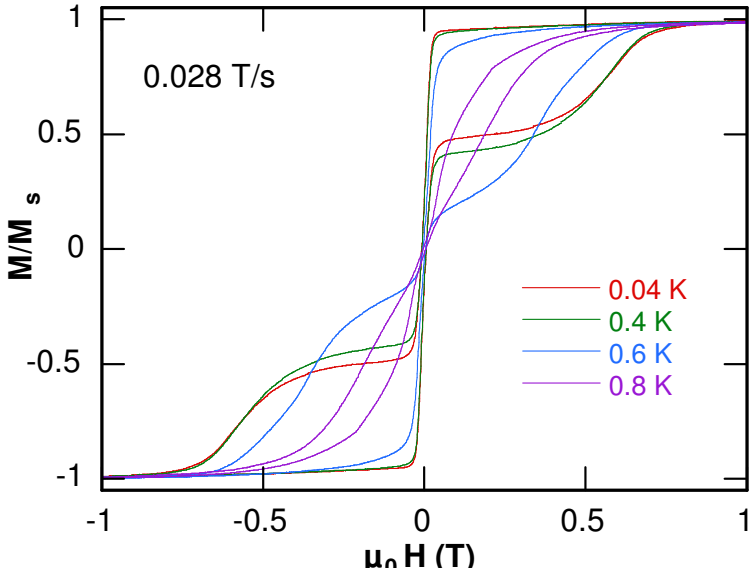

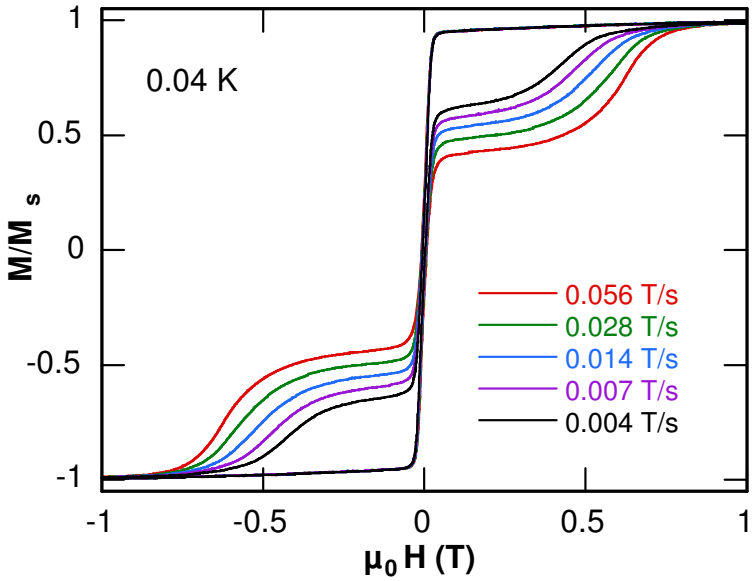

Loops are dominated by the large steps at zero field = fast tunneling rates

-- consistent with low symmetry and significant E value.

-- T_B is smaller than for higher–symmetry Mn_4 SMMs i.e. although D is larger and thus U is larger, the U_{eff} is smaller due to the low symmetry!

Cf: axial

Mn_4 - Si

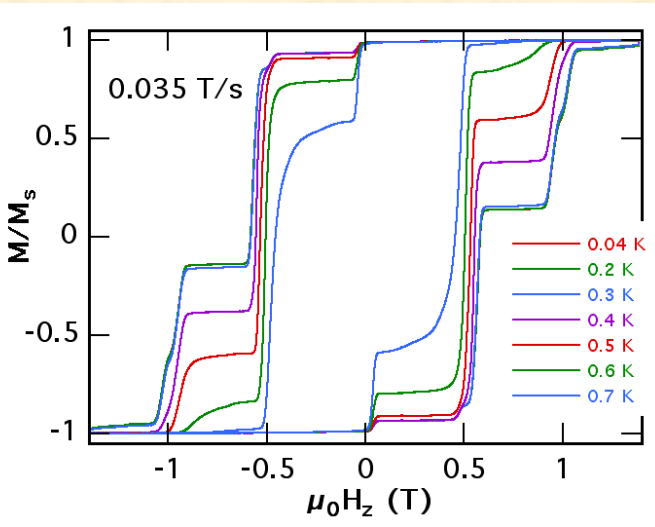

N. Aliaga-Alcalde, W. Wernsdorfer, S.Hill. G. Christou, et al., *JACS*, 2002, *126*, 12503

Synthesis of $[Mn_4O_3Cl_4(O_2CEt)_3(py)_3]$ (NA3 or Mn4Pr)

$[Mn_3O(O_2CEt)_6(py)_3](ClO_4)$

↓ Me_3SiCl in MeCN

$[Mn_4O_3Cl_4(O_2CEt)_3(py)_3]$

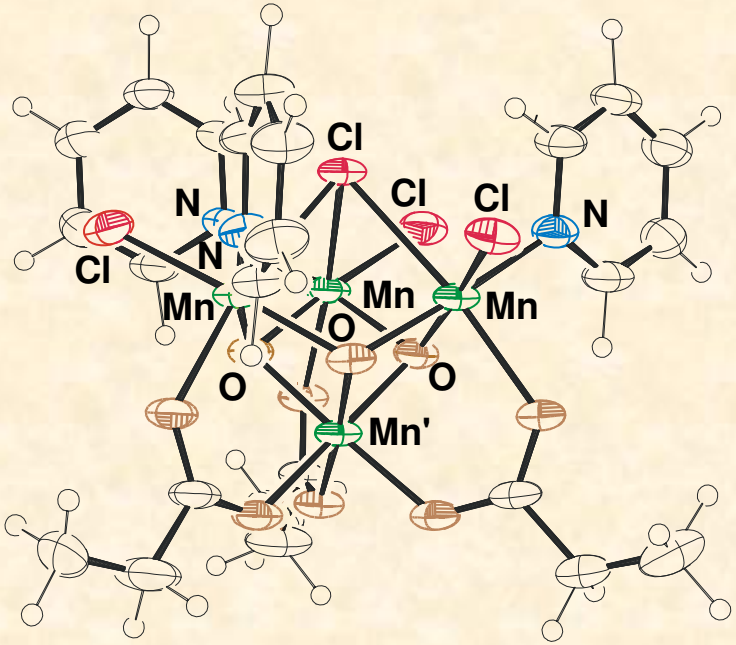

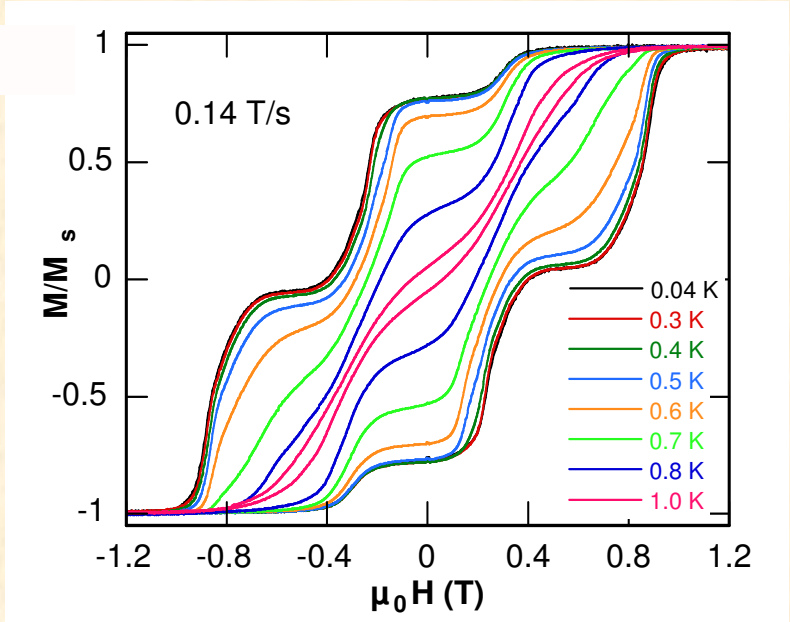

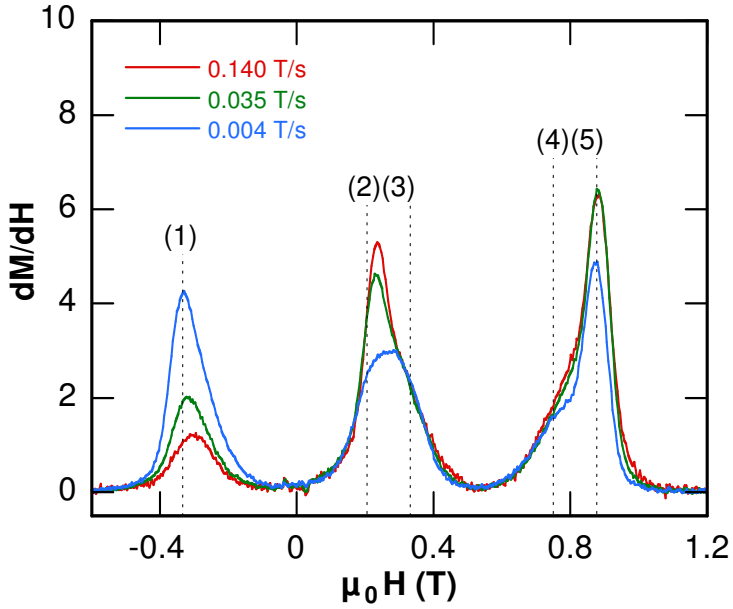

Supramolecular Dimers of Mn_4 SMMs:

Exchange-biased Quantum Tunneling of Magnetization

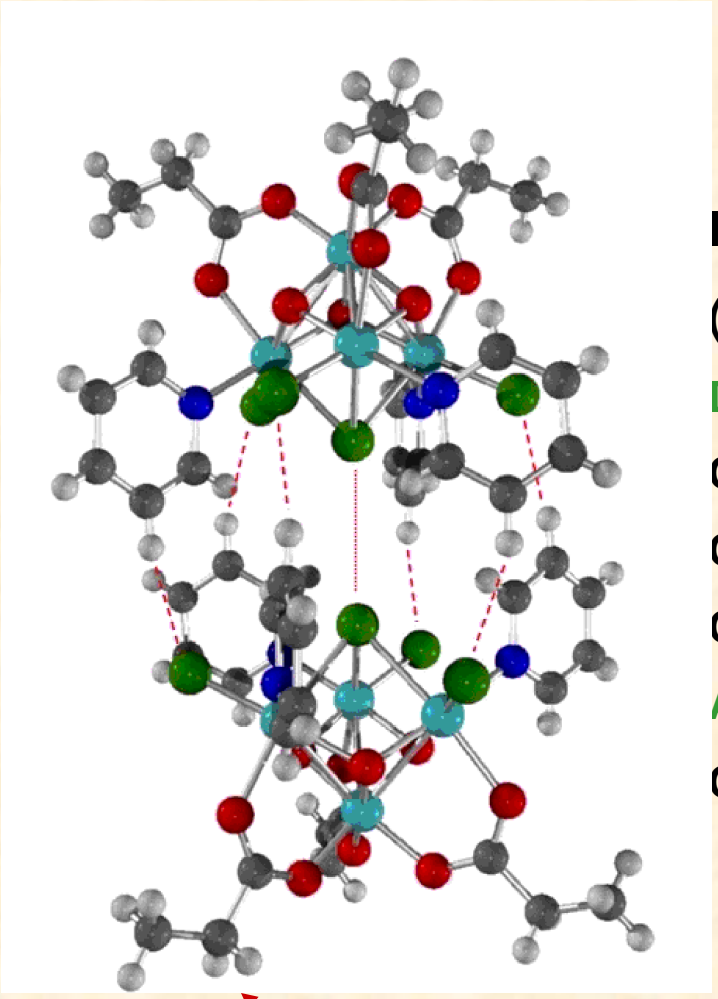

Pr group

$[Mn_4Pr]_2$

Hexagonal R3(bar)

(S_6 symmetry)

Distances

C…Cl 3.71 Å

C-H…Cl 2.67 Å

Cl…Cl 3.86 Å

Angle

C-H…Cl 161.71°

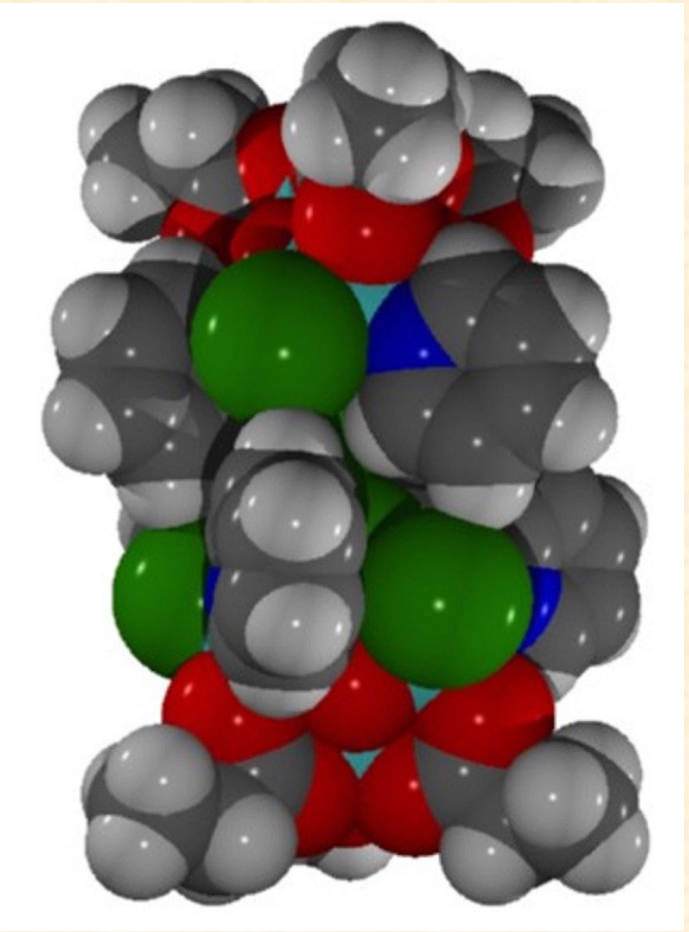

W. Wernsdorfer, N. Aliaga-Alcalde, D. N. Hendrickson, and G. Christou, *Nature*, 2002, 406-409

Quantum Tunneling in an $[Mn_4]_2$ dimer of SMMs

using $[Mn_4Pr]_2 \cdot MeCN$ (NA3)

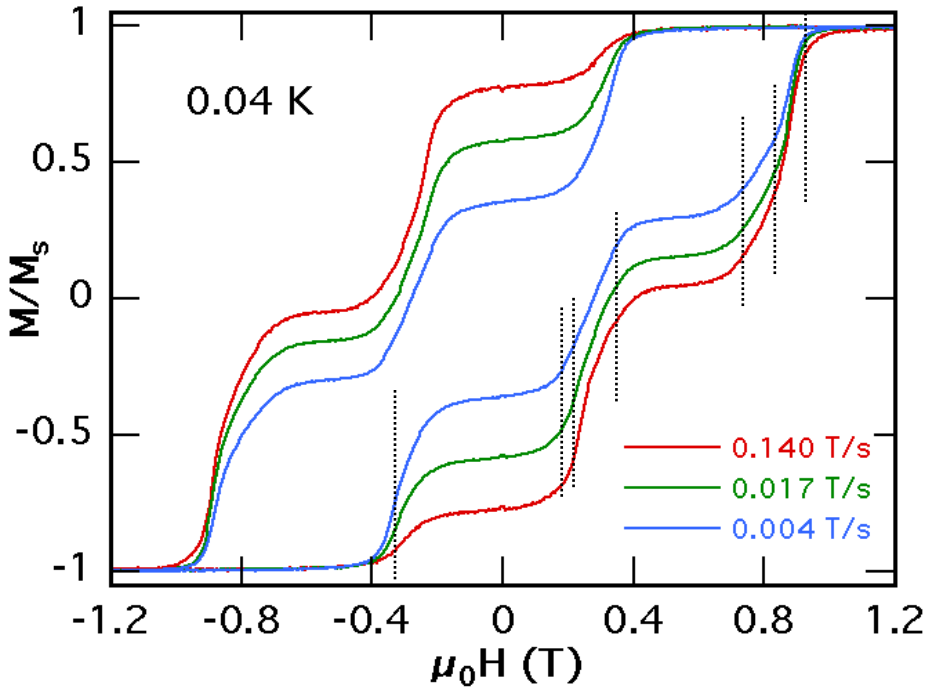

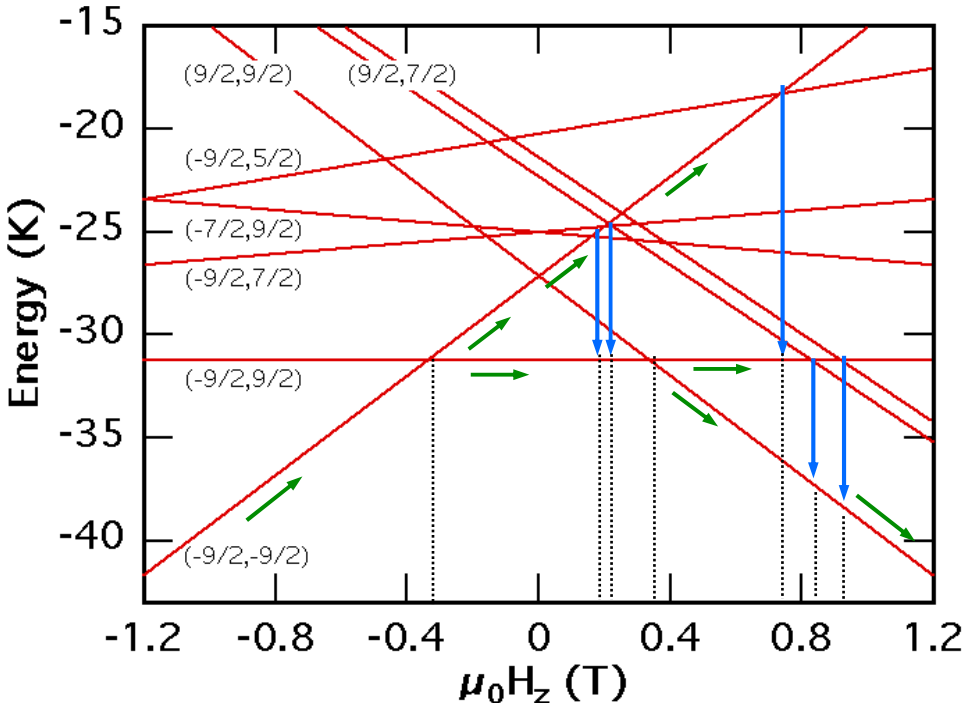

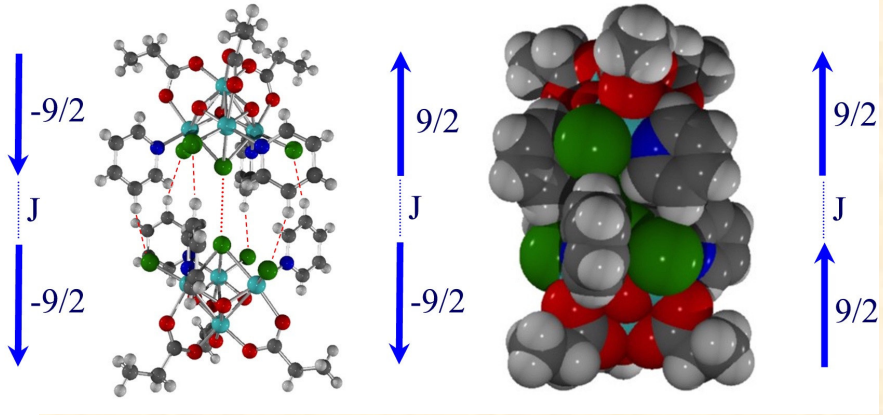

$D = -0.50\ cm^{-1} = -0.72\ K$

$J_{intra} = -0.07\ cm^{-1} = -0.1\ K$

W. Wernsdorfer, N. Aliaga-Alcalde,
D. N. Hendrickson & G. Christou
Nature 2002, *416*, 406

Derivatives of $[Mn_4O_3Cl_4(O_2CR)_3(py\text{-}p\text{-}R')_3]_2$ Dimers

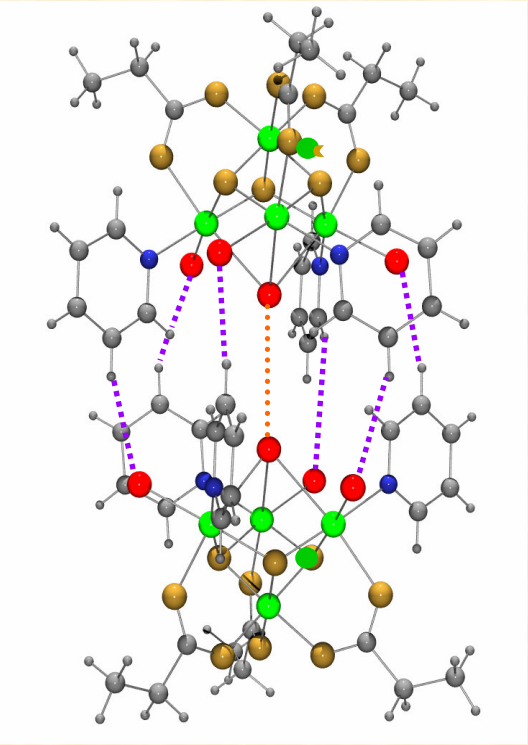

Nuria Aliaga-Alcalde

	R= Me (Ac) R'= H	R= Et (Pr) R'= H	R= Et (Pr) R'= H	R=Et (Pr) R'= D
Space Group	R3bar	R3bar	R3bar	R3bar
Temp(°C)	118	130	173	173
Solvent in the crystal	NA2 MeCN	NA3 MeCN	NA11 hexane	NA3-D MeCN
(Å) Cl ··· Cl	3.739(6)	3.878(5)	3.712(5)	3.844(7)
(Å) Cl ··· C	3.600	3.706	3.664	3.721
(°) C-H··· Cl	158.15	158.00	151.94	157.36
(Å) Mn^{III} ···Mn^{III}	7.630	7.788	7.622	7.750
		Nature	*Science*	

Variation of Exchange-bias and Fine-structure in $[Mn_4]_2$ SMM Dimers

$[Mn_4Ac]_2 \cdot MeCN$
3.739(6)Å

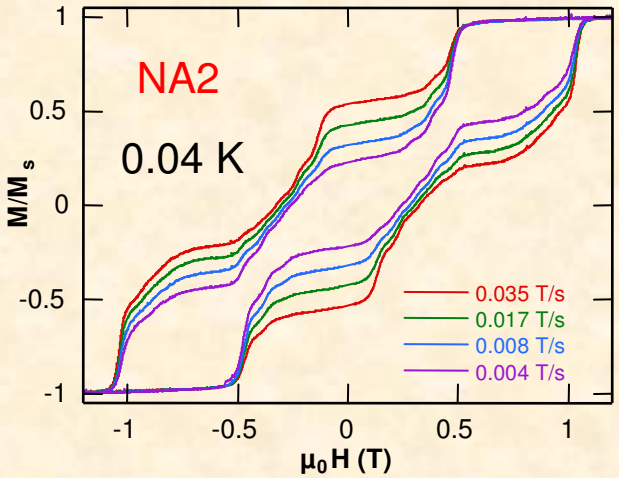

$[Mn_4Pr]_2 \cdot MeCN$ *(Nature)*
3.878(5)Å

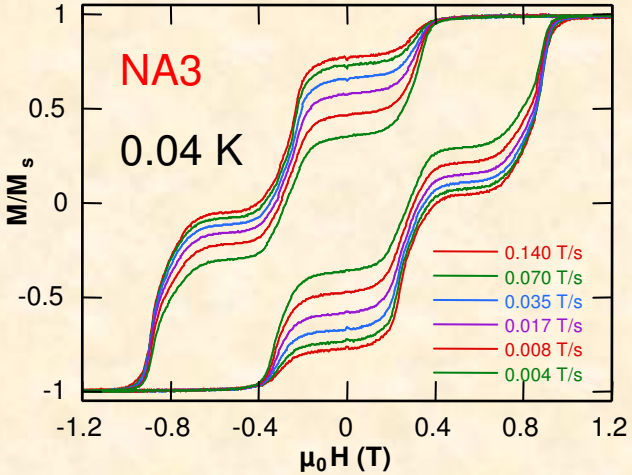

$[Mn_4Pr]_2 \cdot$ hexane *(Science)*
3.712(5)Å

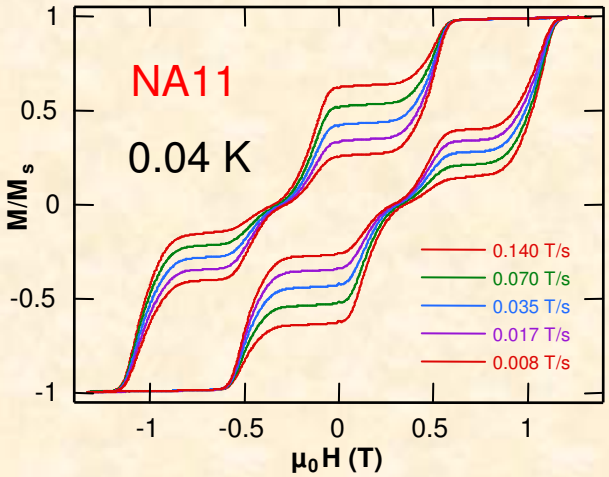

Two effects:

1) **Variation in exchange-bias (J_{intra})**

2) **Variation in fine structure (J_{inter})**

The properties of $[Mn_4]_2$ are very sensitive to the ligands and the solvent in the crystal

Hysteresis evidence for inter-dimer exchange interactions

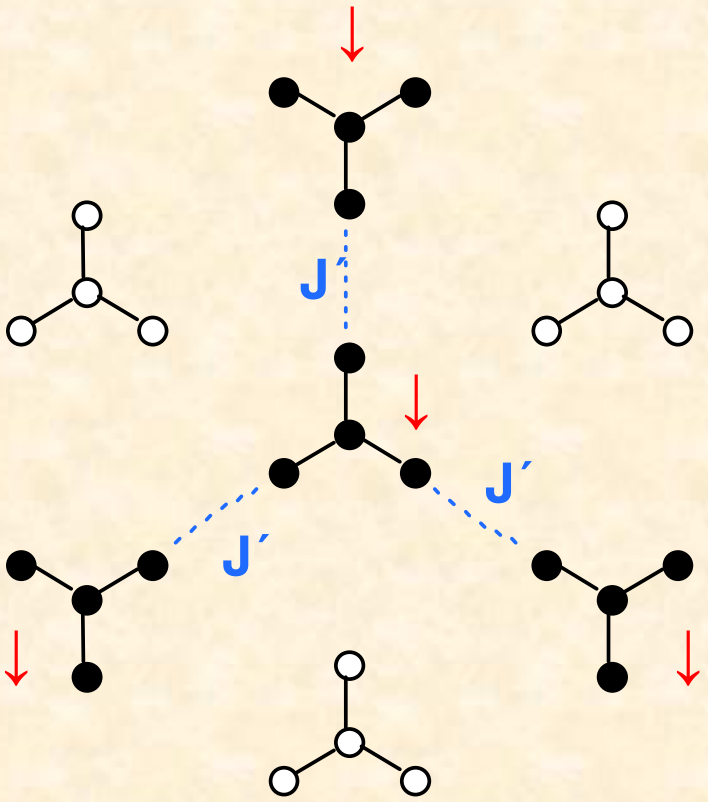

View down S_6 axes

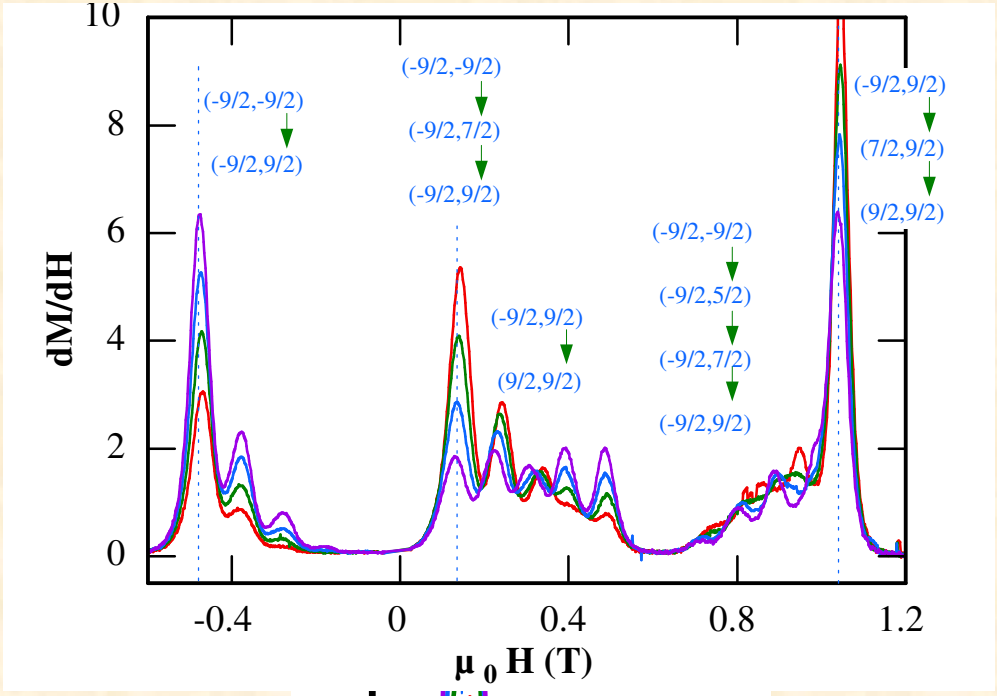

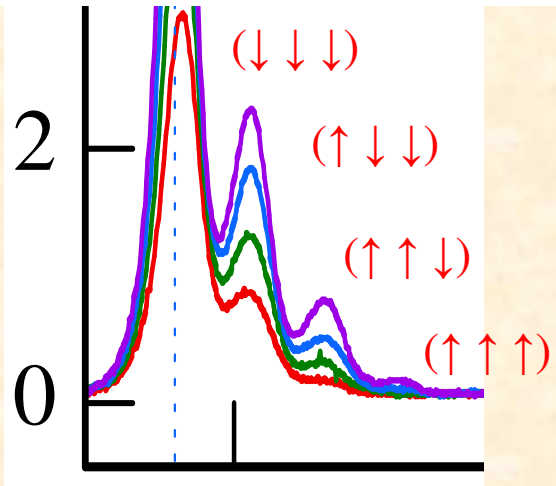

R. Tiron, W. Wernsdorfer, N. Aliaga-Alcalde, and G. Christou, *Phys. Rev. B* 2003, *68*, 140407(R)

Quantum Superpositions in Exchange-coupled $[Mn_4]_2$ Dimers

J_z J_x, J_y -- with $[Mn_4Pr]_2 \cdot$ hexane (NA11)

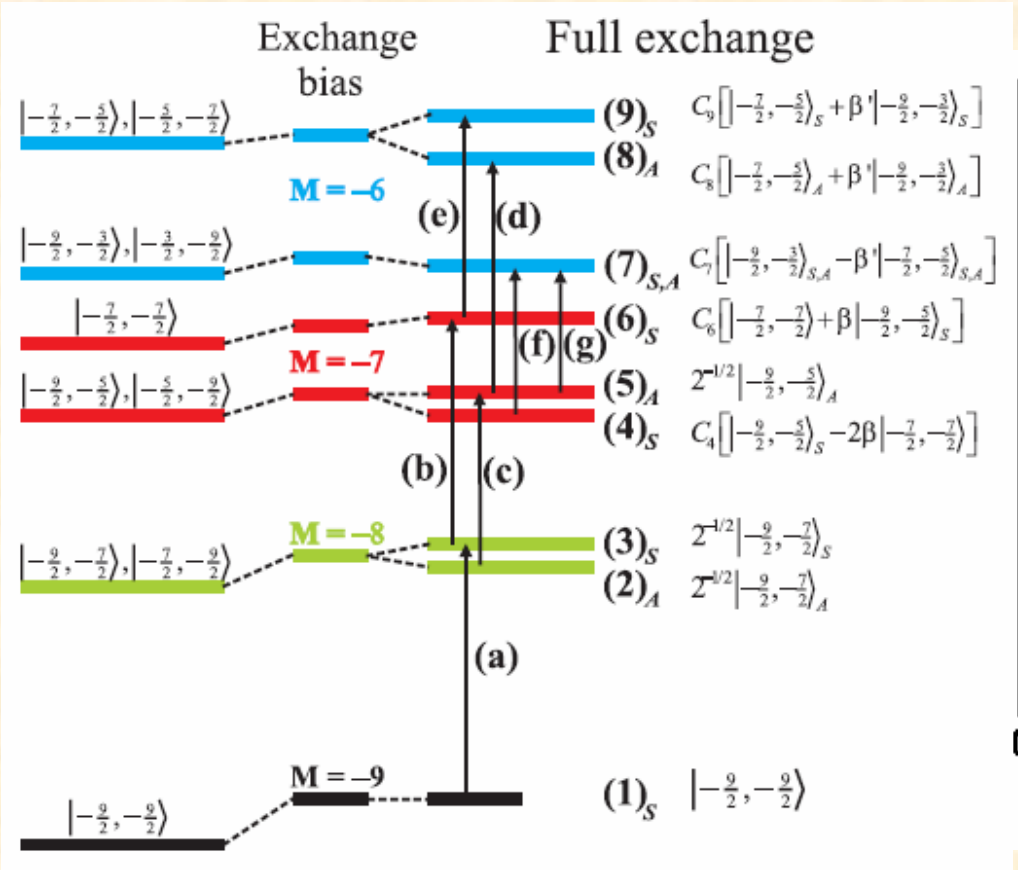

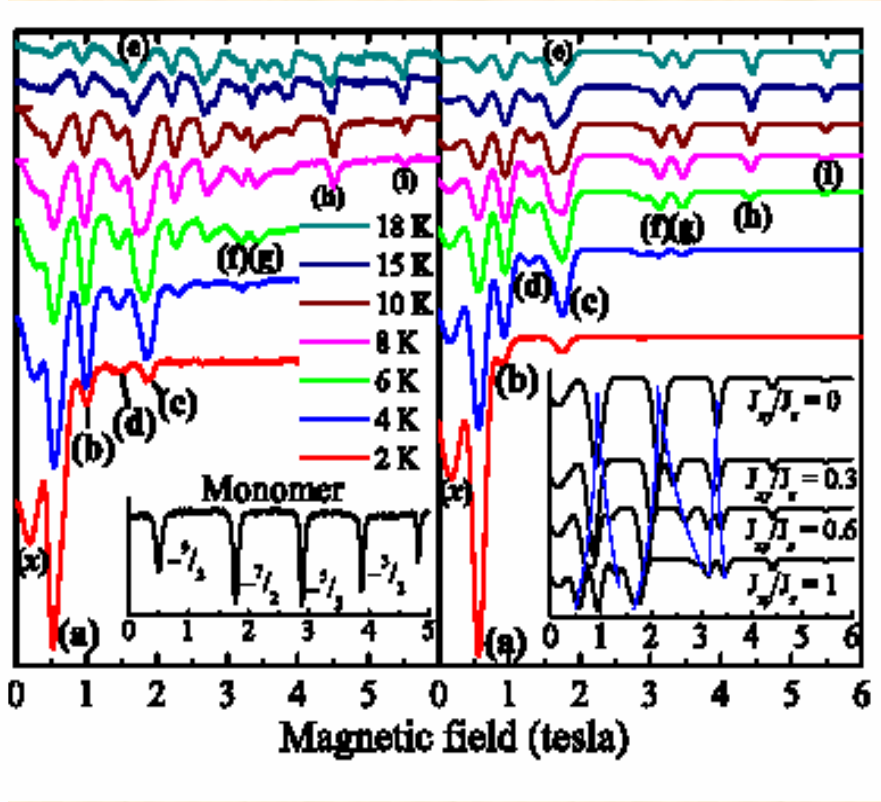

S. O. Hill, R. S. Edwards, N. Aliaga-Alcalde and G. Christou, *Science* 2003, *302*, 1015